THE JOURNAL OF PHYSICAL CHEMISTRY B

ARTICLE

pubs.acs.org/JPCB

Steered Molecular Dynamics Simulations of the Electron Transfer Complex between Azurin and Cytochrome c_{551}

Anna Rita Bizzarri

Biophysics and Nanoscience Centre, CNISM, Facolta' di Scienze, Università della Tuscia, Largo dell'Università, I-01100 Viterbo, Italy

ABSTRACT: The unbinding properties of the transient complex between the electron transfer proteins azurin and cytochrome c_{551} have been investigated by steered molecular dynamics simulations by pulling four different atoms of cytochrome c_{551}. The atoms to be pulled have been chosen to closely match the conditions of a previous experimental study by atomic force spectroscopy. The temporal evolution of the distance between different couples of atoms of the intermolecular hydrogen bonds and of the unbinding force have been analyzed for the various setups and by applying seven different pulling speed values. The observed variability in the response of the system has been traced back to the occurrence of different pathways during the unbinding process. Furthermore, an analysis of the unbinding force as a function of the pulling speed analyzed in the framework of the thermally activated model has allowed the extraction of the dissociation rate constant at equilibrium. These results have been discussed in connection with the transient character of the system and with the available experimental data by atomic force spectroscopy.

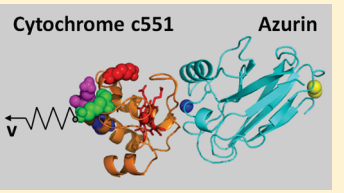

INTRODUCTION

Electron transfer (ET) proteins usually form complexes with a transient character reflecting high dissociation rate constants (up to 10^4 s^{-1}) and ensuring a rapid turnover.[1,2] These proteins possess the further capability to recognize different partners with a rather high degree of specificity.[3] All these features make ET−protein-based complexes particularly intriguing from both fundamental and applicative points of view. Indeed, the study of ET complexes deserves a high interest in the perspective to enlighten molecular features of biorecognition processes, especially in comparison with complexes characterized by tight binding, high affinity, and long lifetimes, such as antigen−antibody and ligand−receptor pairs.[1,4] On the other hand, the ET capability of these complexes makes them suitable to be exploited in applicative fields to build bionano-devices or biosensors with reversible binding.[5]

Here, we have focused our attention on the transient complex formed by the copper protein azurin (AZ) and the heme protein cytochrome c_{551} (C551) from *Pseudomonas aeruginosa*; an exchange of electrons between these two partners has been demonstrated in vitro.[6] Both AZ and C551 have been separately investigated by several approaches to elucidate their ET properties in connection with their dynamical and spectroscopic features even when conjugated to inorganic substrates or nanoparticles (e.g., gold, silver, ITO).[7−15]

Since the structure of the AZ−C551 complex is not known, we have recently applied a computational docking approach to predict the structure of this complex starting from the crystallographic data of the individual partners.[16] The found best structure for the AZ−C551 complex was then used to design an atomic force spectroscopy (AFS) experiment to investigate the unbinding process between AZ and C551.[17] Briefly, the tip of an AFM apparatus has been functionalized with C551 and brought into contact with a gold substrate charged with AZ molecules to form a complex between the biomolecules. Then, an unbinding processes was induced by retracting the tip from substrate. The forces measured in correspondence of the unbinding event at a given rate of applied force, i.e., the so-called loading rate, have been analyzed in the framework of the Bell−Evans model.[18,19] This has allowed the determination of a dissociation rate constant of 14 s^{-1} and an energy width barrier of 0.14 nm, for an individual complex, with slightly lower values being obtained when AZ was anchored to a functionalized instead of a bare gold substrate.[17,20,21]

Here, to complement the AFS study of the AZ−C551 complex, with details at atomic level, we have applied steered molecular dynamics (SMD), a computational approach in which the MD simulations are carried out while a spring, bound to one atom of the system, is pulled at a constant speed to induce the unbinding between the partners.[22,23] The motion of the two sulfurs of the AZ disulfide bridge has been frozen to mimic the anchoring of AZ through its disulfide bridge to the gold substrate in the AFS experiments. Furthermore, since C551 was covalently bound to the AFM tip through a short linker targeting the amino groups of the exposed lysine residues, the spring has been attached to the nitrogen of lateral amino group of one the available lysine residues of C551,[17,20] leading to four different setups. For each one, simulations with seven different pulling speeds in the range 0.0001−0.01 nm/ps have been carried out. In this respect, we note that the pulling speed of SMD simulations is generally orders of magnitude higher than that used in AFS (μ/s range), and then the resulting time scale is much faster than the typical time of AFS experiments.[24−28] Indeed, the unbinding process is often completed within hundreds of picoseconds. However, SMD can provide relevant information to understand the molecular mechanisms regulating the unbinding processes.[22]

Received: August 21, 2010
Revised: December 24, 2010

dx.doi.org/10.1021/jp107933k | *J. Phys. Chem. B* XXXX, XXX, 000–000

The analysis of the unbinding data indicates that the removal of C551 from AZ can follow different pathways varying with the pulled atoms. This can be put into relationship to the transient character of the AZ−C551 complex or to the complexity of the energy landscape whose exploration can affect the determination of the unbinding properties. Furthermore, the unbinding force as analyzed in the framework of the thermally activated model has allowed the determination of the dissociation rate whose value can be compared with the related data from AFS experiments.

COMPUTATIONAL METHODS

System Preparation. The initial coordinates of the AZ−C551 complex were taken from a previous docking study performed by starting from the structures of component proteins.[20] MD simulations were carried out using the GROMACS 4.05 package,[29] including the GROMOS96 43a1 force field.[30] for the proteins and the SPC/E model for water.[31] The copper active site was modeled by following the procedures developed in previous MD works.[7,32] By taking into account that the copper ion of AZ is coordinated by three strong equatorial ligands (two nitrogens from His46 and His117 and one sulfur from Cys112) and two weaker axial ligands (sulfur from Met121 and the backbone oxygen of Gly45), it was covalently bound to N^{δ} of His46 and His117 and S^{γ} of Cys112. The partial charge of the copper charge was fixed to 0.33 e; the partial charges of N^{δ} of both His46 and His117 were −0.58 e, while the partial charge of S^{γ} of Cys112 was fixed at −0.40 e. (for other details see the ref 32). The used force field parameters for the copper active site of AZ was checked by calculating the vibrational modes of the covalent bond between the copper ion and the sulfur of Cys112 by using the method presented in refs 33, 34. These modes have been then compared with the lines of the resonant Raman spectrum of AZ. The found good agreement among the simulated and the experimental vibrational modes lines supports the reliability of the used force field. In this respect, we mention that a collection of different sets of parameters developed for the active site of copper proteins is available in the literature for the various force fields (e.g., see refs 35−37).

The heme group of C551 was covalently bound to three ligands: two sulfurs from Cys12 and Cys15, respectively, and one nitrogen from His16. Atomic charges and all angles and bonds involving the heme site were fixed as the parameters present in Gromos96; the charge of iron was set to 0.40 e and it is the same used in ref38. All ionizable residues of both proteins, with the exception of copper and heme ligands, were assumed to be in the ionization state corresponding to pH 7.0.

The complex was centered in a fixed-volume rectangular box with dimension 14.901 × 5.980 × 6.487 nm^3, filled with water molecules. The box dimension along the x axis was fixed large enough to allow the unbinding of the complex in a wide range of pulling speed values (see below). Solvent molecules whose distance from any atom of the solute molecules was less than 0.23 nm were deleted. To ensure the neutrality of the system, five water molecules were replaced by five chlorine counterions. The final hydrated system contains 2048 protein atoms and 16 799 water molecules. LINCS algorithm was used to constrain the bond lengths.[39] Short-range electrostatic and van der Waals forces, with a cutoff radius of 0.9 nm, were calculated for all pairs of a neighbor list, updated every 10 steps, with nearest-image distances less 1 nm. Electrostatic interactions were calculated by the particle mesh Ewald (PME) method.[40,41] For the calculation

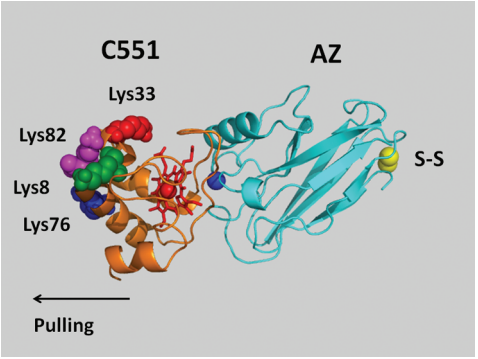

Figure 1. Molecular graphic representation of starting configurations of the AZ−C551 complex. The copper ion of AZ is represented in blue, while the sulfur atoms involved in the disulfide bridge of AZ are in yellow. The porphyrin skeleton and the iron of C551 are in red. The four lysine residues of C551 involved in the pulling process: setup 1, Lys8 (green); setup 2, Lys33 (red); setup 3, Lys76 (blue); setup 4, Lys82 (magenta).

of the reciprocal sum, the charges were assigned to a grid in real space with a lattice constant of 0.12 nm using fourth-order cubic spline interpolation. An energy minimization of 500 steps using the steepest descent method was followed by a 400 ps MD run with harmonic constraints. Successively, the system initially set at 50 K was heated by increasing the temperature up to 300 K in 500 ps by steps of 5 K. A MD run of 3 ns was performed to equilibrate the system by applying periodic boundary conditions, with a step size of 2 fs, at constant temperature and volume (NVT ensemble);[42] these conditions were chosen to match those required for SMD. The relaxation of the system from its initial structure and its final stability was checked by monitoring the root mean square displacement (rmsd), the root mean square fluctuations (RMSF), the gyration ratio of the complex, and the Cu−Fe distance; the results were very similar to those obtained from other runs carried out in the NPT ensemble (i.e., at constant pressure and temperature). We found that the system was relaxed within the first 2 ns of the run and was stable for longer times. The dynamical properties during the last 1 ns time were taken as reference for the system in equilibrium. The structure averaged over the last 100 ps of the run was taken as the starting configuration for SMD simulations (see Figure 1). Figures were created with Pymol.[43]

Steered MD. The SMD of the AZ−C551 complex was carried out by using a setup which closely mimics that used in AFS experiments.[17,20] In particular, the motion of the two sulfurs of the AZ disulfide bridge was kept frozen during the run, to take into account that AZ molecules were anchored to a gold substrate through the disulfide bridge (directly or through the use of spacers). The binding of C551 to the AFM tip through the nitrogen of the amino groups from lysine residues was modeled by taking into consideration that C551 possesses eight lysine residues: Lys8, Lys10, Lys21, Lys28, Lys33 Lys49, Lys76, Lys82 (see Figure 1). From the docking model of the AZ−C551 complex,[16] it comes out that Lys49 is directly involved in the interaction with AZ, while Lys10 and Lys 21 are rather close to the interface region. Accordingly, the anchoring of C551 to the tip through one of these three residues is expected to prevent the formation of a complex and then they were not included in the list of pulled atoms. Furthermore, Lys8 is expected to give rise to results similar to those of Lys10. On such a basis, we chose as pulled atoms the nitrogen from the lateral chain of the following

dx.doi.org/10.1021/jp107933k |J. Phys. Chem. B XXXX, XXX, 000–000

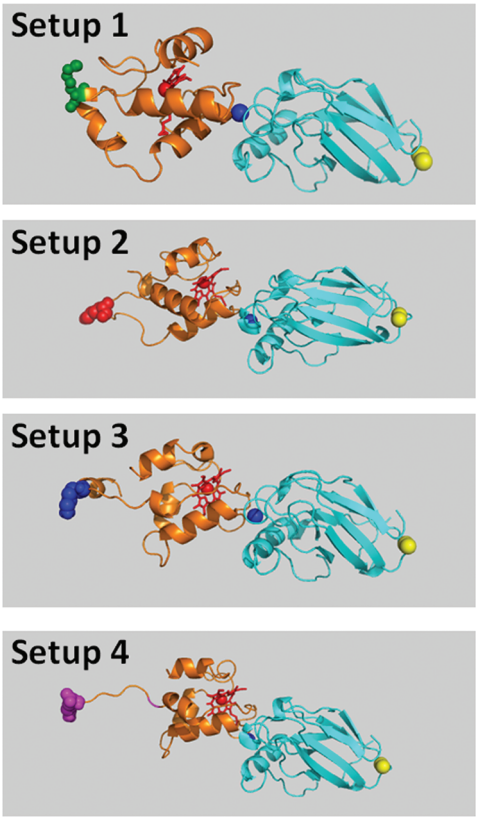

Figure 2. The structures of the complex after 10 ps of SMD run for the four setups. The same representations as in Figure 1 are used.

lysines: Lys8 (setup 1), Lys28 (setup 2), Lys76 (setup 3), and Lys82 (setup 4) (see Figure 1).

To each selected atom of C551, a time-dependent external force was applied by pulling the spring bound to the select atom with a constant speed v:[24,31]

$$F = -k[x_{pull}(t) - x_{pull}(0) - vt] \quad (1)$$

where k is the spring constant, and $x_{pull}(t)$ and $x_{pull}(0)$ are the positions of the pulled atom at the time t and at the initial time, respectively; the speed was applied along the negative direction of x (see Figure 1). For each setup, seven values of pulling speed were applied: 0.001, 0.003, 0.005, 0.01, 0.03, 0.05, and 0.1 nm/ps. These values were chosen in order to obtain the complete unbinding within 3 ns in all the cases. We note that the slowest pulling speed was about 3 orders of magnitude faster than the experimental one.[17] Simulations with faster speeds were also carried out; however, the occurrence of a large and immediate unfolding prevented the complete unbinding with both the proteins within the box. For each speed, five different MD runs were performed by changing the starting velocities. The value of k was fixed at $k = 400$ kJ/mol/nm^2 (corresponding to 0.668 N/m), being in the same range of those usually used in SMD studies to induce unbinding between the partners in a complex.[24,25,27] We mention that the elastic constant of the spring used in the AFS experiments on the AZ/C551 complex had a nominal value of $k = 0.03$ N/m.

RESULTS AND DISCUSSION

Unbinding of the AZ−C551 Complex. Figure 2A−D shows the snapshot of the AZ−C551 complex for the four setups after 300 ps of run carried out with a pulling speed of 0.01 nm/ps. A partial unfolding of C551 in the region close to the pulled atom occurs in all the cases, while the structure of AZ is practically unaffected by the pulling. Such an unfolding is much more evident for the setups 3 and 4, in which the pulled atom is close to the terminal region of the protein. An opposite trend with an unfolding of AZ together with a preservation of the structure of C551 has been observed by using a reverse setup in which the disulfide group of AZ has been pulled, while keeping fixed the related pulled atom of C551 (not shown). Generally, the occurrence of some unfolding during the pulling to induce the unbinding is rather common to the SMD runs of biomolecular complexes, especially at high pulling speed.[27]

By a visual inspection of the trajectories for longer times, we found that the partial unfolding stops before the occurrence of the effective unbinding process which takes place; successively, slightly different paths have been observed in the various setups. To quantitatively describe both the unfolding and unbinding processes, we have monitored the time evolution of the distances between specific couples of atoms in the complex. In particular, to investigate the protein−protein interface, we have followed the distance (indicated as D_1) between the C_α(Met44) of AZ and the C_α (Asn64) of C551 and the distance (D_2) between the C_α (Met64) of AZ and the C_α(Gln53) of C551. Furthermore, the unfolding of C551 has been monitored by analyzing the distance (D_3) between the C_α(Phe114) of AZ and the pulled atom of C551 of the corresponding setup and the distance (D_4) between the C_α (Ser159) and the C_α (Val181) of C551.

Figure 3 shows the time evolution of the D_1-D_4 distances for the four setups from simulation with a pulling speed of 0.01 nm/ps. Generally, the four analyzed distances exhibit a markedly different trend in time with smaller changes among the various setups. To put into evidence the deviations of these distances from the value obtained from the system at equilibrium (i.e., without any applied force), we have marked the time at which the corresponding distance deviates of more than two standard deviations from the average equilibrium value (see the circles in Figure 3). These times are rather different among the various setups and even among the analyzed distances. This means that each system is characterized by a different temporal evolution.

By separately analyzing the D_1-D_4 distances, we note that D_1 and D_2 follow almost the same qualitative trend in all the setups. In particular, they remain close to the initial value for a rather long time, ranging from 250 to 700 ps and then they linearly increase. The difference between D_1 and D_2 is more marked for the setups 3 and 4, with respect to the setups 1 and 2. The observed constant trend is indicative that the protein−protein interface is preserved and the two partners are forming a complex before the occurrence of the effective unbinding process. Additionally, the observation of a linear trend during the unbinding can be put into relationship to the establishment of a drift regime in which C551 is removed from AZ at a constant velocity.

The distance D_3 remains close to the initial value for a time interval ranging from about 50 to 300 ps for the various setups, and then it linearly increases up to reach a maximum. By taking into account the fact that D_3 monitors the distance between two atoms inside C551, such behavior reflects some unfolding of the C551 protein, during the pulling process. The successive decreases of D_3 down to a value close to the initial one in all the setups indicates that the pulled protein undergoes some structural relaxation, leading to a significant decrease in its extension along the pulling direction. Interestingly, both the maximum

dx.doi.org/10.1021/jp107933k |J. Phys. Chem. B XXXX, XXX, 000–000

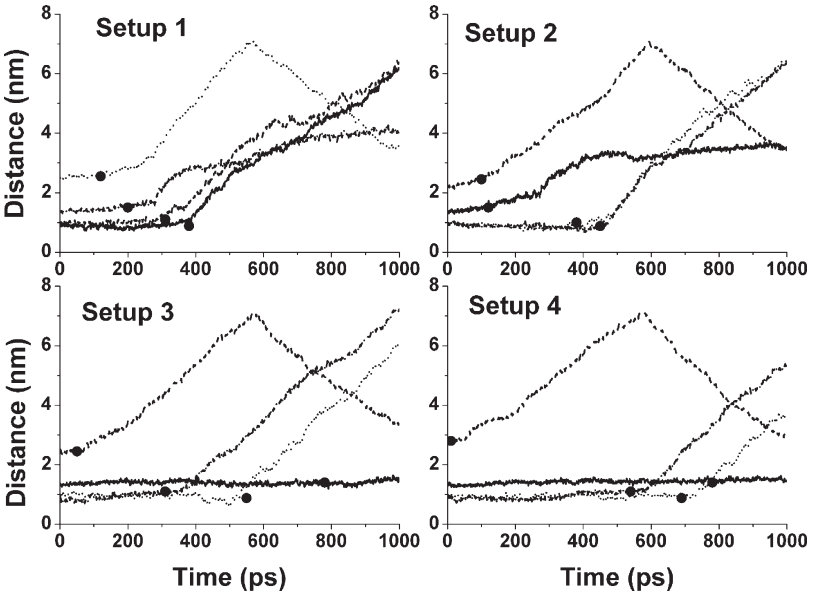

Figure 3. Temporal evolution of the distance D_1 between the C_α (Met44) of AZ and the C_α (Asn64) of C551 (continuous line, black), the distance D_2 between the C_α (Met 64) of AZ and the C_α (Gln53) of C551 (dashed line, red), the distance D_3 between the C_α Phe114) of AZ and the pulled atom of C551 (dotted line, green), and the distance D_4 between the C_α (Ser159) and the C_α (Val181) of C551 (dashed-dot line, blue) for the four setups by a pulling speed of 0.01 nm/ps. Circles mark the times at which the corresponding distance exceeds, for the first time, the equilibrium value (i.e., the value related to the system without any applied force) given by the $\langle D_i \rangle + 2\sigma_i$, where $\langle D_i \rangle$ are the average and σ_i the standard deviation values, respectively, for the corresponding distance D_i.

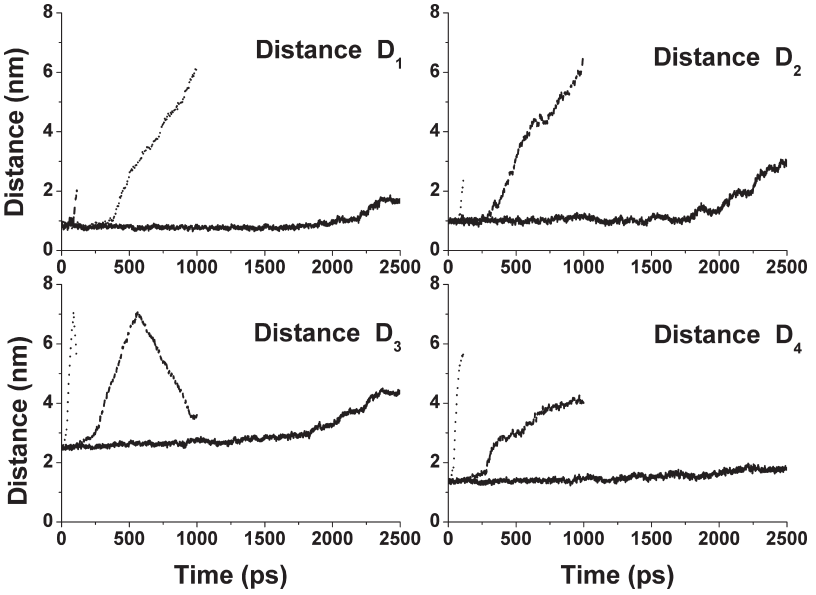

Figure 4. Temporal evolution of the distances D_1, D_2, D_3, and D_4 for the setup 2 by using three different pulling speed values: 0.001 nm/ps (continuous line), 0.01 nm/ps (dashed line), and 0.1 nm/ps (dotted line).

extension of the protein and the time required to reach it are practically the same for all the setups. This is rather surprising, even in the light of the fact that the unfolding process depends on the pulled atom. Notably, the time corresponding to the maximum is generally before the establishment of the unbinding process.

The distance D_4, which gives information on the unfolding of C551 complementarily to those provided by D_3, follows rather different trends for the various setups. Indeed, after an in initial time interval during which D_4 is practically unchanged, it increases for setups 1 and 2, while it remains substantially constant for setups 3 and 4. This means that the involved portion of C551 undergoes some structural changes during the pulling process only for setups 1 and 2, while it is stable in the other cases. Finally, we remark that only slight differences in the D_1-D_4 trends are observed by varying the initial conditions.

Figure 4 shows the evolution of the D_1-D_4 distances, for the setup 1 by applying speed values of 0.001, 0.01, and 0.1 nm/ps. Since the unbinding occurs within shorter times as far as faster speeds are applied, the temporal windows are progressively

dx.doi.org/10.1021/jp107933k |J. Phys. Chem. B XXXX, XXX, 000–000

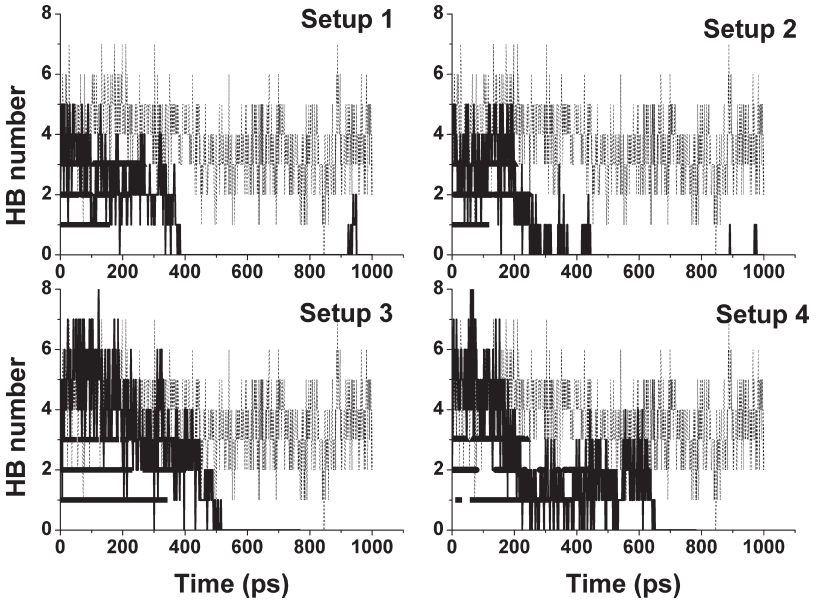

Figure 5. Temporal evolution of the HB number formed between AZ and C551 under the application of the force with a pulling speed of 0.01 nm/ps and without any applied force (dashed lines) for the four setups (continuous lines). The time at which the three most frequent HBs are marked: HB-A (triangles), Gly116 (AZ) and Gln57 (C551); HB-B (circles), Thr61 (AZ) and Gln53 (C551); HB-C (squares), Asn50 (C551) and Asn42 (AZ).

shorter for faster pulling speed values. At the lowest speed (0.001 nm/ps), all the distances remain close to the initial values for long times, exhibiting an increase at the end of the simulation. Furthermore, they do not reveal marked differences among the various setups. Notably, for this pulling speed, the trend of D_3 does not exhibit a maximum, consistently with the fact that the C551 protein does not undergo to a significant unfolding during the unbinding process. This supports the hypothesis that even in AFS experiments, whose pulling speed are much faster, no unfolding of the involved proteins takes place.

At variance, at the highest speed value of 0.1 nm/ps, the distance D_3 shows a trend in time rather similar to that observed for 0.01 nm/ps and previously discussed, with a large increase followed by a decrease after reaching maximum. The maximum extension of the C551 protein does not depend on the pulling speed value, supporting the fact that it depends on the structural properties of the protein. Generally, these results on the time evolution of the D_1-D_4 distances show that the unbinding process of C551 from AZ might occur in concomitance with a partial unfolding of the region close to the pulled atom which drastically decreases when low pulling speed values are applied. The evidence that D_1-D_4 evolve by following different trends for the various setups is consistent with the unbinding taking place through different breaking sequences, which may lead to different unbinding paths.

Some more information about the evolution of the protein−protein interface during the pulling process can be obtained by monitoring the intermolecular hydrogen bonds (HBs). Figure 5 shows the total number of HBs formed between the two partners as a function of time, for the four setups with a pulling speed of 0.01 nm/ps (continuous lines). For comparison, the total number of HBs recorded for the system in equilibrium in a time interval of 1000 ps is also shown (dashed lines in Figure 5). For all the setups, at the beginning of the run, the HB number fluctuates around the initial value of between 5 and 7, and then it decreases to zero within times varying from 400 to 650 ps depending on the setups. Such a behavior can be put into relationship to the progressive removal of the two proteins with a concomitant weakening of their interaction. Setup 4 maintains the protein−protein HB network for longer times, with respect to the other setups, likely due to the occurrence of a more marked unfolding which slows the unbinding process.

A detailed analysis of the HBs formed during a 1000 ps run for the system at equilibrium has revealed 22 different HBs between AZ and C551, with a large part of these HBs being only occasionally found, while nine of them have a frequency higher than 34%. The time at which the three most frequent HBs, labeled as HB-A, HB-B, and HB-C, are detected is also marked in Figure 5 (see also the related legend). We note that three analyzed HBs follow a different trend in time with a similar behavior being observed even for different initial conditions. This provides further support to the hypothesis that the unbinding process proceeds following different paths when different atoms are pulled.

These results about the distances between couples of atoms and about the interproteins HBs during the SMD runs show that the unbinding of the AZ−C551 complex takes place by following slightly different pathways when different atoms are pulled. Accordingly, it can be hypothesized that the two partners are kept together by a collection of bonds not strongly hierarchically organized. In other words, the sequence of the rupture could change when the pulling conditions are modified. In this respect, we mention that rather well-defined unbinding paths have been observed for other complexes investigated by SMD.[24,25] In principle, the observed behavior for the AZ−C551 complex could be due to its transient character, which may involve the formation of a so-called encounter complex constituted by an ensemble of energetically similar complexes of the two partners.[1] Accordingly, the bonds keeping together these complexes are expected to be almost equivalent in energy.

Unbinding Force Analysis. As already mentioned, the application of an external force to induce the unbinding of two

dx.doi.org/10.1021/jp107933k |J. Phys. Chem. B XXXX, XXX, 000–000

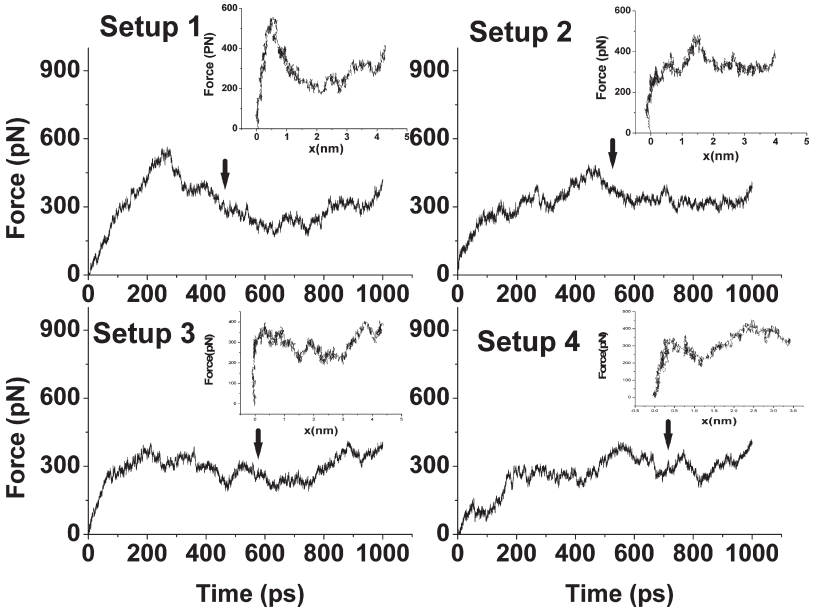

Figure 6. Temporal evolution of the applied forces (see eq 1) during the SMD with a pulling speed of 0.01 nm/ps, for the four setups. The arrows mark the time at which the unbinding is just completed. Inset: the evolution of the same applied forces (see eq 1) as a function of the distance between the pulled atom and the spring (i.e., the distance D_3), for the four setups.

biomolecular partners forming a complex leads to a nonequilibrium process with a concomitant deformation of the energy landscape. In particular, upon applying a force, a decrease of the energy barrier from the bound to the unbound state is usually induced.[18] This decrease gives rise to an alteration of both the kinetics and thermodynamical properties of the unbinding process. The properties at equilibrium can be, however, extracted from these nonequilibrium data, under appropriate conditions and by applying suitable theoretical models.[18,19,44] From force spectroscopy experiments on complexes, the measured unbinding force plotted as a function of logarithm of the loading rate follows a linear trend, allowing determination of the dissociation rate constant and the width of the energy barrier in the framework of the Bell−Evans model.[19] One of the main assumptions of this model is that the applied force gives rise to an activated regime characterized by a fastening of the unbinding process arising from the slight decrease of the energy barrier.[18,44] In SMD simulated experiments, the stronger applied force could induce a significant reduction of the energy barrier or even a cancellation of it.[45] Accordingly, an activated, a diffusive, or even a drift regime can be established depending on the strength of the applied force.[23,39]

Figure 6 shows the time evolution of the applied force (see eq 1) at the pulling speed of 0.01 nm/ps for the four setups. At very short times (less than 1 ps), a rapid, linear increase independent of the pulling speed and on the setup has been observed. Such a behavior finds a correspondence with Hooke's law, as expected from the dominant contribution from first two terms in eq 1. Successively, the force increases more slowly with an almost linear trend; the slope becomes higher as far as faster pulling speeds are applied, as expected from eq 1. After about 200 ps of the run, a decrease of the force takes place followed by a rather variable trend with time significantly different for the various setups. The same qualitative behavior of the force has been observed for different initial conditions. By taking into account the previous results on the distances, the temporal course of the force can be approximately divided into three regions. During the first part, the force increases, leading to a progressive weakening of the protein−protein interactions, and a concomitant partial unfolding of the pulled molecules for high pulling speed values takes place. However, the two partners are still forming a complex. During the second part, the effective unbinding process of the complex takes place and a decrease of the applied force is observed; the arrows mark the time at which the unbinding is found to be completed (see also below). Finally, in the last part, the applied force induces a further removal of C551 from AZ with the approaching to the diffusive regime which is limited by the border of the simulation box. Notably, the different shapes assumed by C551 after the partial unfolding could be responsible for the different force trend observed in the last part of the run for the various setups. However, clear, direct evidence for the occurrence of the unbinding cannot be extracted from the force time course. In this respect, we remark that the maximum of the force does not correspond to the unbinding, as instead suggested for some SMD runs of biomolecular complexes.[24,26,27] On the other hand, in atomic force spectroscopy experiments, the occurrence of the unbinding process reflects into a clear jump in the force plotted as function of the distance between the AFM tip and the substrate (related to the distance between the partners), where the two biomolecules are bound. For a more direct comparison between experimental and simulated data, we have plotted the force as a function of the distance between the pulled atom and the spring (D_3). Such a parameter well-describes the related position between the C551 and AZ during the run (see the inset in Figure 6). From the plots shown in the inset of Figure 6, it comes out that a close correspondence between the trend of the force as a function of time and that as a function of the distance occurs for all the setups. Such a behavior is confirmed even for the other loading rate values. Such a behavior suggests that during the pulling the system is maintained not too far from equilibrium.

Since we are interested in determining the value of the unbinding force, i.e., the force value just in correspondence of

dx.doi.org/10.1021/jp107933k |J. Phys. Chem. B XXXX, XXX, 000–000

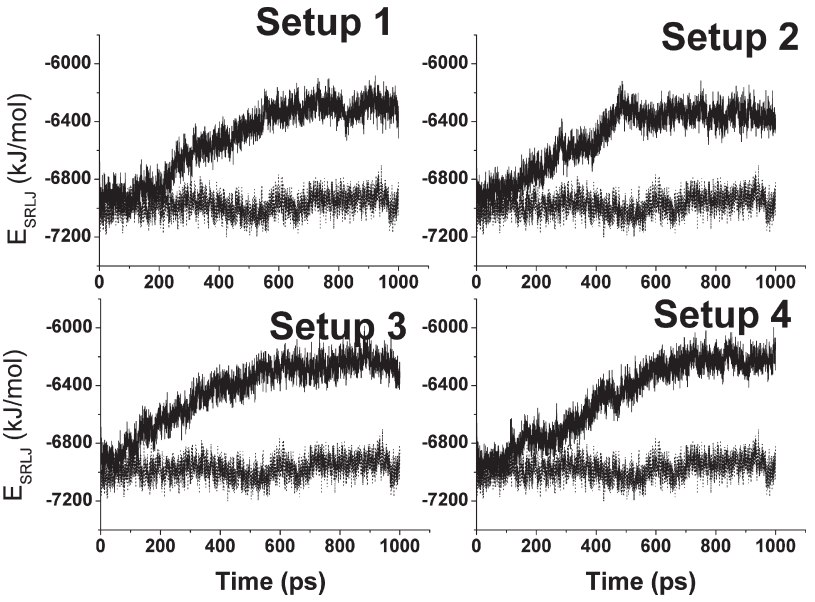

Figure 7. Temporal evolution of the short-range Lennard-Jones energy, E_{SHLJ}, for the protein−protein interaction for the four setups for simulations with a pulling speed of 0.01 nm/ps. For comparison, the same quantity for the system in equilibrium, i.e., without any applied force, is shown (dashed gray lines).

the unbinding, to extract some information on the kinetic properties on the unbinding process of the complex, we are looking for a suitable criterion to determine the time at which the unbinding process has been just completed. With such an aim, we have analyzed the temporal behavior of the protein−protein energy. In particular, we have focused our attention on short-range Lennard-Jones energy, E_{SRLJ}, which provides information even about slight changes in the interaction between the partners. The time evolution of E_{SRLJ} is shown in Figure 7, for the four setups from simulations with a pulling speed of 0.01 nm/ps; for comparison, the evolution of the system in equilibrium is also shown for all the setups (dashed lines). In all the cases, E_{SRLJ} shows an almost constant trend close to that of the system in equilibrium. Successively, the E_{SRLJ} energy increases by reaching an almost constant value, with the related fluctuations being of the same order as those observed for the system in equilibrium. The time at which the E_{SRLJ} deviates from the initial values, as well as the duration of the transient period, is slightly different for the various setups. A similar qualitative behavior has been observed for the simulations with other pulling speeds or initial conditions. From these results, we have assumed that the unbinding is just completed when E_{SRLJ} reaches the new equilibrium value; the force at which this new equilibrium value has been just reached has been assumed to be the unbinding force. We have verified that at the time corresponding to the unbinding, both the distances D_1 and D_2 exceed the 1.3 nm value.

Figure 8 shows the unbinding force of the AZ−C551 complex as a function of the logarithm of the pulling speed for the four setups, with each value being averaged over five simulations obtained with different initial conditions. An increasing trend of the unbinding force with the pulling speed is observed for all the setups, with a significant deviation from a linear regime at higher pulling speed being registered. At pulling speed values lower than 0.01 nm/ps, the increase of the unbinding force with the logarithm of the loading rate can be satisfactorily described by a linear trend. Accordingly, the related data have been analyzed in terms of a thermally activated regime, for which the applied force

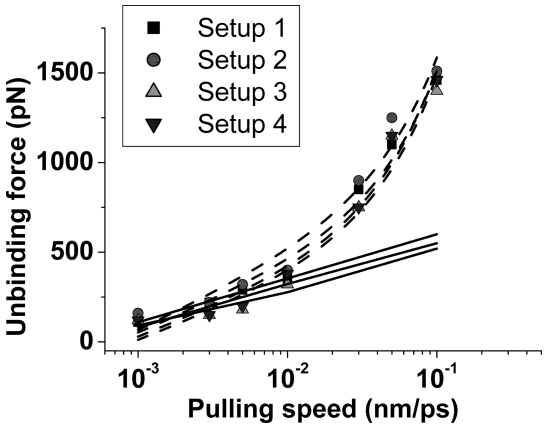

Figure 8. The unbinding force, extracted from the SMD runs, as a function of the logarithm of the pulling speed for the four setups. Continuous lines: fit through eq 2 of data with pulling speed less than 0.01 nm/ps. Dashed line: fit through eq 3 of data with pulling speed in the whole range. For the extracted parameters see Table 1.

to the system yields a slight decrease of the energy barrier separating the bound from the unbound state.[46] More specifically, in the framework of the one-dimensional memory-free diffusion model for unbinding processes, the unbinding force can be then described by the following expression:[26,27]

$$F_{unb} = \frac{k_B T}{x_\beta} \ln\left(\frac{k v x_\beta}{k_o k_B T}\right) \quad (2)$$

where x_β is the width of the barrier potential, k_o is the dissociation rate constant at equilibrium, k_B is the Boltzmann constant, T is the absolute temperature, v is the pulling speed, and k is the elastic constant of the spring. A fit of the unbinding force data for $v < 0.01$ nm/ps by eq 2 has allowed the calulation of the x_β and k_o parameters for all the setups (see the Table 1). We found that the energy barrier width, x_β, is about 0.04−0.05 nm for all the setups,

dx.doi.org/10.1021/jp107933k |J. Phys. Chem. B XXXX, XXX, 000–000

Table 1. Parameters Extracted from Two Different Fits of the Unbinding Force Plotted as a Function of the Logarithm of Pulling Speed, Given in Figure [8,a]

setup	x_β (nm)	$k_o \times 10^9$ (s^{-1})	$\gamma \times 10^9$ (N s/m)	x_β (nm)	$k_o \times 10^9$ (s^{-1})
1	0.04	1.9	7.8	0.02	2.9
2	0.04	1.7	7.5	0.02	2.8
3	0.05	2.8	8.6	0.03	5.3
4	0.05	3.0	9.1	0.03	4.9

[a] The x_β and k_o parameters reported in columns 2 and 3 have been then determined by using eq 2 and unbinding force data obtained with pulling speed lower than 0.01 nm/ps. The γ, x_β, and k_o parameters respectively reported in columns 4, 5, and 6 have been then determined by using eq 3 and unbinding force data for all the pulling speed values.

such a value being in agreement with those estimated for biomolecular complexes when fast pulling regimes are applied.[47,48] We also note that x_β is slightly higher for the setups 3 and 4 with respect to the setups 1 and 2. This suggests that the geometrical properties of the energy barrier to be overcome is different when the pulling takes place along different directions. Furthermore, we note that the x_β values are different from those extracted, at single molecule level, from the AFS studies for which x_β is within the interval 0.1−0.14 nm.[17,20] This might be due to some modification of the proteins structures and properties occurring in the real system likely induced by the immobilization procedures.[20,21]

The estimated dissociation rate at equilibrium, k_o, has been found to be on the order of 10^9 s^{-1} for all the setups. Such a value is likely higher than the values expected for transient complexes, for which it is generally assumed to be higher than 10^4 s^{-1}.[1] On the other hand, it should be mentioned that a reliable quantitative evaluation of k_o from the SMD data has been questioned in ref 26. Nevertheless, the estimated values for k_o allow comparison of the results from the various setups. The fact that k_o is slightly lower for setups 1 and 2 with respect to setups 3 and 4 suggests that the kinetic properties of the complex and then the energy landscape features are different by pulling different atoms. This could be interpreted in terms of either a different modulation of the energy barrier upon applying a force to different atoms or to the exploration of different regions of the energy landscape. Both of these aspects should require further investigations.

For faster pulling speeds, the higher applied force induces a further decrease of the energy barrier, which may determine a diffusive and/or a drift regime.[46] In this case, the resulting motion is a friction-dominated term with an expected linear dependence of the unbinding force on the pulling speed v: $F_{unb} = \gamma v$, where γ is the friction coefficient. Accordingly, the trend of the unbinding force as a function of the whole range of the pulling speed can be described by the following expression:

$$F_{unb} = \frac{k_B T}{x_\beta} \ln\left(\frac{k v x_\beta}{k_o k_B T}\right) + \gamma v \qquad (3)$$

where the first term is related to an activated thermally regime (see eq 2), while the latter takes into account the friction-dominated regime. The fit of all the data in Figure 8 by eq 3 provides a good description for all the setups in the whole range of pulling speed (see the continuous lines), with the obtained fitting parameters being also reported in Table 1 (columns 4−6). The energy barrier width, x_β, is about 0.02−0.03 nm for all the setups. Such a value is lower with respect to the previous fit; however, it is again slightly higher for the setups 3 and 4 with respect to the setups 1 and 2. The dissociation rate at equilibrium, k_o, is again on the order of 10^9 s^{-1} for all the setups, with the same trend among the setups as previously observed .

Concerning the friction coefficient γ, reported in Table 1, we note that slightly higher values have been obtained for setups 3 and 4 with respect to setups 1 and 2. This can be put into relationship to some differences in the diffusion properties of the C551 in the various setups, likely due to its different shape after the unfolding occurring at the higher pulling speeds. The friction coefficient values can be compared with the experimental one derived from the Einstein relationship $D = k_B T/\gamma$, where D is the diffusion coefficient, k_B is the Boltzmann constant, and T is the absolute temperature. Using for D the value determined for cytochrome c of about 8.4×10^{-11} m^2/s, a value for γ of 5×10^{-11} N s/m can be obtained;[49] such a value is slightly higher than that extracted from our SMD data.

In summary, the data show that the kinetic properties of the complex slightly vary when different pulling atoms are pulled. This could be indicative of a different deformation of the energy barrier to be overcome when different atoms are pulled, or alternatively, that different regions of the energy landscape are explored depending on the pulled atoms, as already mentioned. Under the assumption of the latter hypothesis, it should be remarked that the energy hypersurface of biomolecular systems is characterized by a large complexity with the existence of many nearly isoenergetic minima.[50−52] Accordingly, the energy barriers to be overcome during the unbinding processes, and then their widths, height, etc., could vary when different regions of the energy landscape are explored as a consequence of pulling along different directions. In other words, proteins systems are characterized by some glasslike features with an high impact on many properties.[53]

However, irrespectively, of the possible origin, some caution in the analysis of the AFS experiments on biomolecular complexes in which the data commonly arise from a collection of slightly different geometrical configuration should be exerted. Indeed, the setup is not completely controlled, since the biomolecules are anchored to the AFM tip or substrate through residues put throughout the protein surface. Accordingly, unbinding processes are induced by applying a force along different directions. This could provide an explanation for the large variability observed in the unbinding data by different experimental techniques in a single molecule regime.[46]

CONCLUSIONS

It was found that the unbinding process of the transient complex between AZ and C551 as investigated by SMD takes place through a sequence of steps varying with the pulling conditions, suggesting the existence of different unbinding pathways. Such variability, on one hand, could be a peculiarity of the transient character of the complex; on the other, it could be ascribed to the complexity of the energy landscape, a partially explored region during the unbinding process. Furthermore, the behavior of the unbinding force as a function of the pulling speeds has been successfully analyzed in the framework of thermally activated model, allowing the determination of the energy barrier width and the dissociation rate, at equilibrium. The slight differences observed on the extracted values of the parameters for various setups indicate some dependence of the pulling conditions.

dx.doi.org/10.1021/jp107933k |J. Phys. Chem. B XXXX, XXX, 000–000

These results provide some useful suggestions to investigate the biorecognition process and even to analyze the experimental data obtained by AFS or from other single molecule techniques.

■ ACKNOWLEDGMENT

I would like to thank Prof. Salvatore Cannistraro for his continuous support, fruitful discussion, and suggestions.

■ REFERENCES

(1) Crowley, P. B.; Ubbink, M. *Acc. Chem. Res.* **2003**, *36*, 723–730.
(2) Nooren, I. M. A.; Thornton, J. M. *J. Mol. Biol.* **2003**, *325*, 991–1018.
(3) Janin, J. Kinetics and thermodynamics of protein−protein interactions. In *Protein−Protein Recognition*; Oxford University Press: New York, 2000.
(4) Schreiber, G.; Haran, G.; Zhou, H. X. *Chem. Rev.* **2009**, *109*, 839–860.
(5) Willner, I.; Katz, E. *Angew. Chem., Int. Ed.* **2000**, *39*, 1180–1218.
(6) Cutruzzolà, F.; Arese, M.; Ranghino, G.; van Pouderoyen, G.; Canters, G. W.; Brunori, M. *J. Inorg. Biochem.* **2002**, *88*, 353–361.
(7) Arcangeli, C.; Bizzarri, A. R.; Cannistraro, S. *Biophys. Chem.* **1999**, *78*, 247–257.
(8) Farver, O.; Lu, Y.; Ang, M. C.; Pecht, I. *Proc. Natl. Acad. Sci. U.S.A.* **1999**, *96*, 899–902.
(9) Nar, H.; Messerschmidt, A.; Huber, R.; van de Kamp, M.; Canters, G. W. *J. Mol. Biol.* **1991**, *221*, 765–772.
(10) Webb, M. A.; Loppnow, G. R. *J. Phys. Chem. A* **1999**, *103*, 6283–6287.
(11) Cimei, T.; Bizzarri, A. R.; Cannistraro, S.; Cerullo, G.; De Silvestri, S. *Chem. Phys. Lett.* **2002**, *362*, 497–503.
(12) Bizzarri, A. R.; Andolfi, L.; Taranta, M.; Cannistraro, S. *Biosens. Bioelectron.* **2008**, *24*, 204–209.
(13) Matsuura, Y; Takano, T.; Dickerson, R. E. *J. Mol. Biol.* **1982**, *156*, 389–409.
(14) Ceruso, M. A.; Grottesi, A.; Di Nola, A. *Proteins.* **2003**, *50*, 222–229.
(15) Bizzarri, A. R.; Bonanni, B.; Costantini, G.; Cannistraro, S. *ChemPhysChem* **2003**, *4*, 1189–1195.
(16) Bizzarri, A. R.; Brunori, E.; Cannistraro, S. *J. Mol. Recogn.* **2007**, *20*, 122–131.
(17) Bonanni, B.; Kamruzzahan, A. S. M.; Bizzarri, A. R.; Rankl, C.; Gruber, H. J.; Hinterdorfer, P.; Cannistraro, S. *Biophys. J.* **2005**, *89*, 2783–2791.
(18) Bell, G. I. *Science* **1978**, *200*, 618–627.
(19) Evans, E. *Annu. Rev. Biophys. Biomol. Struct.* **2001**, *30*, 105–128.
(20) Bonanni, B.; Bizzarri, A. R.; Cannistraro, S. *J. Phys. Chem. B.* **2006**, *110*, 14574–14580.
(21) Bonanni, B.; Andolfi, L.; Bizzarri, A. R.; Cannistraro, S. *J. Phys. Chem. B* **2007**, *111*, 5062–5075.
(22) Rief, M.; Grubmueller, H. *ChemPhysChem.* **2002**, *3*, 255–261.
(23) Israelewitz, B.; Gao, M.; Schulten, K. *Curr. Opin. Struct. Biol.* **2001**, *11*, 224–230.
(24) Bayas, M. V.; Schulten, K.; Leckband, D. *Biophys. J.* **2003**, *84*, 2223–2233.
(25) Curcio, R.; Caflisch, A.; Paci., E. *Protein Sci.* **2005**, *14*, 2499–2514.
(26) Heymann, B.; Grubmueller, H. B. *Chem. Phys. Lett.* **1999**, *303*, 1–9.
(27) Neumann, J.; Gottschal, K. E. *Biophys. J.* **2009**, *97*, 1687–1699.
(28) Zhang, Y.; Tan, H.; Lu, Y.; Jia, Z.; Chen, G. *FEBS Lett.* **2008**, *582*, 1355–1361.
(29) Lindahl, E.; Hess, B.; van der Spoel, D. *J. Mol. Model.* **2001**, *7*, 306–317.
(30) Van der Spoel, D.; Lindahl, E.; Hess, B.; Groenhof, G.; Mark, A. E.; et al. *J. Comput. Chem.* **2005**, *26*, 1701–1710.
(31) Berendsen, H. J. C.; Grigera, J. R.; Straatsma, T. P. *J. Phys. Chem.* **1997**, *91*, 6269–6271.
(32) De Grandis, V.; Bizzarri, A. R.; Cannistraro, S. *J. Mol. Recogn.* **2007**, *20*, 215–226.
(33) Bizzarri, A. R.; Cannistraro, S. *Chem. Phys. Lett.* **2001**, *349*, 503–510.
(34) Cimei, T.; Bizzarri, A. R.; Cerullo, G.; De Silvestri., S.; Cannistraro, S. *Biophys. Chem.* **2003**, *106*, 221–231.
(35) Sugiyama, A.; Takamatsu, Y.; Nishikawa, K.; Nagao, H.; Nishikawa, K. *Int. J. Quantum Chem.* **2006**, *106*, 3071–3078.
(36) Rajapandian, V.; Hakkim, V.; Subramanian, V. *J. Phys. Chem. B* **2010**, *114*, 8474–8486.
(37) Swart, M. 2002. Density functional theory applied to copper proteins. Ph.D. thesis, Rijksuniversiteit Groningen, Groningen.
(38) Ceruso, M. A.; Grottesi, A.; Di Nola, A. *Proteins* **2003**, *50*, 222–229.
(39) Hess, B.; Bekker, H.; Berendsen, H. J. C.; Fraaije, J. G. E. M. *J. Comput. Chem.* **1997**, *18*, 1463–1472.
(40) Kholmurodov, K.; Smith, W.; Yasuoka, K.; Darden., T.; Ebisuzaki, T. *J. Comput. Chem.* **2000**, *21*, 1187–1191.
(41) Darden, T.; York, D.; Pedersen, L. *J. Chem. Phys.* **1993**, *98*, 10089–10092.
(42) Berendsen, H.; Postma, J.; van Gunsteren, W.; Dinola, A.; Haak., J. *J. Chem. Phys.* **1984**, *81*, 3684–3690.
(43) Guex, N.; Peitsch, M. C. *Electrophoresis.* **1997**, *18*, 2714–2723.
(44) Bizzarri, A. R.; Cannistraro, S. *Chem. Soc. Rev.* **2010**, *39*, 734–749.
(45) Izrailev, S.; Stepaniants, S.; Balsera, M.; Oono, Y.; Schulten, K. *Biophys. J.* **1997**, *72*, 1568.
(46) Rico, F.; Moy, V. T. *J. Mol. Recognit.* **2007**, *20*, 495–501.
(47) Pincet, F.; Husson, J. *Biophys. J.* **2005**, *89*, 4374–4381.
(48) Paeschke, M.; Hintsche, R.; Wollenberger, M. U.; Jin, W.; Scheller, F. *J. Electroanal. Chem.* **1995**, *393*, 131–135.
(49) Frauenfelder, H.; Parak, F.; Young, R. D. *Annu. Rev. Biophys. Biophys. Chem.* **1988**, *17*, 451–479.
(50) Barsegov, V.; Thirumalai., D. *Phys. Rev. Lett.* **2005**, *95*, 168302–168305.
(51) Robert, P.; Benoliel, A. M.; Pierres, A.; Bongrand, P. *J. Mol. Recogn.* **2007**, *20*, 432–447.
(52) Bizzarri, A. R.; Cannistraro, S. *J. Phys. Chem. B.* **2002**, *106*, 6617–6633.
(53) Bizzarri, A. R.; Cannistraro, S. *J. Phys. Chem. B.* **2009**, *113*, 16449–16464.